ELSEVIER

Chemical Engineering Journal 117 (2006) 23–29

Chemical Engineering Journal

www.elsevier.com/locate/cej

CFD simulation of homogeneous reactions in turbulent pipe flows—Tubular non-catalytic reactors

K. Ekambara [a], M.T. Dhotre [b], J.B. Joshi [c,*]

[a] *Department of Chemical & Materials Engineering, University of Alberta, Alberta, Canada T6G 2G6*
[b] *Thermal Hydraulics Laboratory, Nuclear Energy and Safety Department, Paul Scherrer Institute, CH-5232 Villigen PSI, Switzerland*
[c] *Institute of Chemical Technology, University of Mumbai, Matunga, Mumbai 400019, India*

Received 7 September 2005; received in revised form 19 November 2005; accepted 9 December 2005

Abstract

An analysis of turbulent reactive flows in tubular non-catalytic reactors is presented for various reaction orders and rate constants. A CFD model has been developed to predict the flow pattern in pipe flow using low Reynolds number k–ε model. Particular emphasis is placed upon analyzing the phenomena near the wall region. The CFD model has been extended to simulate the axial dispersion phenomena in turbulent regions. Further, the CFD model has been extended to obtain changes in the radial and axial concentration distributions. For the case of thermally neutral reactions and the isothermal conditions, it was observed that the lower order reactions cause a more rapid decrease in the axial concentrations. The effect of Reynolds and Schmidt numbers on the conversion levels is also discussed.

Keywords: Axial dispersion coefficient; Homogeneous reaction; Turbulent region; CFD; Low Reynolds number k–ε model

1. Introduction

Profitable chemical reactions often require critical reaction conditions. In case of fast exothermic or endothermic reactions, large reaction volumes lead to difficulties in controlling the process variables pressure and temperature. Conducting the reaction in small volumes enables not only a proper control, but prevents also severe damages in case of inhomogeneities or instabilities. Thus, it is often advisable to prefer continuous processing to batch processing. The two basic continuous reactor types are the continuous stirred-tank reactor and the tubular plug-flow reactor. Tubular reactors are simple and easy to construct. Furthermore, a narrow residence time distribution can be achieved by turbulent flow conditions. In case of small tube diameters, the geometry allows operation at high pressures. The favorable ratio of surface to volume enhances heat transfer and thus simplifies the adjustment of a desired axial temperature profile. The design and calculation of tubular reactors can cause problems, because fluid mechanics, reaction kinetics and thermodynamics are coupled and difficult to describe mathematically especially in case of reactions with phase transitions. Rates of chemical reactions are best determined in these tubular reactors operated in turbulent regimes to avoid falsification of the true kinetics by diffusion effects. Predictions of concentration profiles in turbulent reactors, where chemical reactions and diffusional effects occur in conjunction, constitute a basic problem of reactor design. Under such flow conditions the general concept of residence time loses meaning because of its non-uniform distribution brought about by the turbulent velocity profiles. In turbulent flows, because of the nature of the momentum profiles, most of the changes occur in a layer in the immediate vicinity of the wall.

The real success of any such analysis depends to a considerable extent on how carefully the eddy diffusivity variation is chosen near the wall. In view of the importance of the accurate description of the velocity profile and eddy viscosity near the wall, an attempt has been made in the present work to employ computational fluid dynamics (CFD). In the recent years, the low Reynolds number k–ε model of turbulence have been widely used in numerical simulations due to their ability of resolving the near wall region. The low Reynolds number k–ε modeling approach incorporates either a wall-damping effect or a direct effect of molecular viscosity, or both, on the empirical constants and functions in the turbulence transport equations. A fairly complete review of the low Reynolds number k–ε model of the

* Corresponding author. Tel.: +91 22 414 5616; fax: +91 22 414 5614.
E-mail address: jbj@udct.org (J.B. Joshi).

1385-8947/$ – see front matter © 2006 Elsevier B.V. All rights reserved.
doi:10.1016/j.cej.2005.12.006

Nomenclature

a	radius of the pipe (m)
c	instantaneous concentration of the tracer
$\bar{c}$	time-averaged concentration of the tracer
C	mean concentration of the tracer, defined in Eq. (19)
C_0	initial concentration of the tracer
$C_{\varepsilon 1}$, $C_{\varepsilon 2}$, C_μ	constants in turbulence models
d	diameter of the pipe (m)
D_{eff}	effective diffusion coefficient, defined in Eq. (15) (m^2/s)
D_{m}	molecular diffusivity, defined in Eq. (16) (m^2/s)
D_{t}	eddy diffusivity, defined in Eq. (17) (m^2/s)
D_{rr}	radial component of turbulent dispersion tensor (m^2/s)
D_{zz}	axial component of turbulent dispersion tensor (m^2/s)
E	term defined in Eq. (8)
f	friction factor
f_1, f_2, f_μ	damping functions used in low Reynolds number k–ε model, terms defined in Eqs. (5)–(7), respectively
k	turbulent kinetic energy per unit mass ($\bar{v}_z^2/2$) (m^2/s^2)
k_n	reaction rate constant
K	constant is defined in Eq. (14)
L	length of the pipe (m)
n	reaction order
p	mean pressure (N/m^2)
r	radial distance (m)
R_{A}	homogeneous rate of reaction of species A
Re	Reynolds number (dU/ν)
R_{T}	turbulent Reynolds number ($k^2/\nu\varepsilon$)
Sc	Schmidt number (ν/D_{m})
Sc_{t}	turbulent Schmidt number ($\nu_{\text{t}}/D_{\text{t}}$)
t	time (s)
u^+	dimensionless velocity ($\bar{v}_z/U$)
u^*	friction velocity ($\sqrt{\tau_0/\rho}$) (m/s)
U	cross-sectional average axial velocity (m/s)
$\bar{v}_z$	time-averaged velocity (m/s)
y	dimensionless radial distance (r/a)
y^+	dimensionless wall distance (yu^*/ν)
z	axial distance along the pipe (m)
z^*	dimensionless axial distance (z/a)

Greek letters

ε	turbulent energy dissipation rate per unit mass ($\bar{v}_z^3/a$) (m^2/s^3)
μ	viscosity (Pa s)
ν	molecular kinematic viscosity (μ/ρ) (m/s)
ν_{t}	turbulent kinematic viscosity, defined in Eq. (4) (m^2/s)
ρ	density (kg/m^3)
σ_{k}	Prandtl number for turbulent kinetic energy
σ_ε	Prandtl number for turbulent energy dissipation rate

turbulent shear flows has been given by Patel et al. [1], Hrenya et al. [2] and Thakre and Joshi [3,4]. Near wall turbulence models or low Reynolds number models, which attempt to describe the relative influence of molecular and turbulent viscosities have been developed for single-phase flows. Thakre and Joshi [3] have analyzed 12 different low Reynolds number k–ε models for the case of a single-phase pipe-flow. For this purpose, they have used four criteria; accurate prediction of the radial variation of axial velocity (compared with experimental data of Durst et al. [5]), the turbulent kinetic energy and the eddy diffusivity and the overall energy balance, i.e., the volume integral of ε must be equal to the energy-input rate (the pressure drop multiplied by volumetric flow rate). Such a stringent criterion was found to be satisfied by Lai and So [6] model (LSO) as shown by Thakre and Joshi [7]. Ekambara and Joshi [8] have successfully used low Reynolds number Lai and So [6] model to predict flow pattern (mean velocity and eddy diffusivity) and used the flow pattern for the prediction of axial mixing in turbulent pipe flows. They have shown excellent agreement between the CFD predictions and the experimental data over a wide range of Reynolds number and Schmidt number.

The objective of this study is to present an analysis of tubular non-catalytic reactors in turbulent flow regimes and to establish the effect of arbitrary reaction orders and various reaction rate constants. Since exact analytical solutions of this problem are impossible to obtain. An attempt has been made in the present work to employ CFD. Effects of various parameters such as, pipe diameter and length, reaction order, reaction constant, Reynolds number, Schmidt number have been investigated. This treatment is directed towards an understanding of the physical structure of the solution by the development of pertinent concentration profiles.

2. Previous work

Bosworth [9] investigated changes in the distribution of residence times due to molecular diffusion. For Poiseuille flows, he has shown the conditions under which either the axial or the radial diffusion could be neglected in evaluating the reaction rate data. The work was extended by Denbigh [10] for second-order reactions. He neglected all the diffusional effects and derived expressions for the conversion of reactants. One of the more comprehensive analyses of first-order reactions in viscous flow was reported by Cleland and Wilhelm [11] in their study of the hydrolysis of acetic anhydride. They used the finite difference numerical technique to examine the effect of the reaction rate constant on point and average concentrations. The results of Bosworth's investigation were also confirmed by them. Krongelb and Strandberg [12] used numerical methods similar to those of Cleland and Wilhelm [11] to investigate the specific example of second-order homogeneous reaction of the recombination of atomic oxygen. Lauwerier [13] presented an analytical solution of the same problem, but the result is so complex that it is difficult to use for any practical applications. Wissler and Schechter [14] extended Lauwerier's [13] analysis to include the case of consecutive irreversible first-order reactions. Vignes and Trambouze [15] conducted a detailed study of the saponifica-

tion of ethyl acetate in laminar flow reactors, incorporating the analysis of both the first- and second-order reactions. Analytical solutions were shown for the two asymptotic cases of plug flow and negligible diffusion, with the intermediate conditions solved by a numerical analysis technique. Hsu [16] solved the identical problem by a quasi-analytical method using the separation of variables technique. His method reduced the numerical work required in the solution of a partial differential equation to that for an ordinary differential equation. Edwards and Saletan [17] conducted an excellent study consisting of segregations effects in pseudo-laminar flow reactors in which they analyzed the lack of conversion or a "slip" due to various reaction orders and velocity profiles, as compared with the plug-flow performance.

All the above investigations have been reported for laminar flows. However, for turbulent pipe flows along with reaction, hardly any information is available in the published literature possibly because of the complexity of the problem. Further prediction of the concentration field in the tubular reactors constitutes one of the fundamental problems in the design of reactor. Theoretical means of predicting the concentration field in such processes are of value both from theoretical and practical points of view. Therefore, it was thought desirable to undertake a systematic investigation.

3. Model formulation

3.1. Modeling of turbulence in pipe flow

For steady, isothermal, incompressible, fully developed pipe flow, the set of governing equations is given as below:

Momentum equation:

$$0 = \frac{1}{r}\frac{\partial}{\partial r}\left(r(\nu+\nu_t)\frac{\partial \bar{v}_z}{\partial r}\right) - \frac{1}{\rho}\frac{\partial p}{\partial z} \tag{1}$$

Transport equation for the turbulent kinetic energy (k):

$$-\frac{1}{r}\frac{\partial}{\partial r}\left(r\left(\nu+\frac{\nu_t}{\sigma_k}\right)\frac{\partial k}{\partial r}\right) = \nu_t\left(\frac{\partial \bar{v}_z}{\partial r}\right)^2 - \varepsilon \tag{2}$$

Transport equation for the turbulent energy dissipation rate (ε):

$$-\frac{1}{r}\frac{\partial}{\partial r}\left(r\left(\nu+\frac{\nu_t}{\sigma_\varepsilon}\right)\frac{\partial \varepsilon}{\partial r}\right) = \frac{C_{\varepsilon 1} f_1 \nu_t \varepsilon}{k}\left(\frac{\partial \bar{v}_z}{\partial r}\right)^2 - \frac{\varepsilon^2}{k}C_{\varepsilon 2} f_2 + E \tag{3}$$

where

$$\nu_t = C_\mu f_\mu \frac{k^2}{\varepsilon} \tag{4}$$

$$f_1 = 1 + \left[1 - 0.6\,\exp\left(-\frac{Re}{10^4}\right)\right]\exp\left(-\left(\frac{R_T}{64}\right)^2\right) \tag{5}$$

$$f_2 = 1 - \frac{2}{9}\exp\left[-\left(\frac{R_T}{64}\right)^2\right] \tag{6}$$

$$f_\mu = 1 - \exp(-0.015y^+) \tag{7}$$

$$E = 2\nu C_{\varepsilon 2} f_2 \frac{\varepsilon}{k}\left(\frac{\mathrm{d}\sqrt{k}}{\mathrm{d}r}\right)^2 + \exp\left(-\left(\frac{R_T}{64}\right)^2\right) \times \left[\left(\frac{7}{9}C_{\varepsilon 2} - 2\right)\frac{\varepsilon}{k}\left(\varepsilon - 2\nu\left(\frac{\mathrm{d}\sqrt{k}}{\mathrm{d}r}\right)^2\right) - \frac{1}{2k}\left(\varepsilon - \frac{2\nu k}{y}\right)^2\right] \tag{8}$$

All the low Re models adopt a damping function f_μ to account for the direct effect of molecular viscosity on the shear stress near the wall (viscous sub-layer and buffer zone). It may be noted that the wall functions used in connection with the standard k–ε model ($f_\mu = 1$) are usually applied in a region $y^+ > 30$. Further, in the low Reynolds number k–ε model, the function f_2 is introduced primarily to incorporate the low Reynolds effect in the destruction term of ε. The important criterion for the function f_2 is that, it should force the dissipation term in the ε equation to vanish at the wall. At high Reynolds number flows, remote from the wall, the function f_1 asymptotes to the value of one in accordance with the high Reynolds number form of the model. The k–ε model parameters are: $C_\mu = 0.09$, $C_{\varepsilon 1} = 1.35$, $C_{\varepsilon 2} = 1.8$, $\sigma k = 1$ and $\sigma_\varepsilon = 1.3$.

Boundary conditions:

$$\text{At the centre,}\quad \frac{\partial \bar{v}_z}{\partial r} = 0;\qquad \frac{\partial k}{\partial r} = 0;\qquad \frac{\partial \varepsilon}{\partial r} = 0$$
$$\text{At the wall,}\quad k = 0;\qquad \varepsilon = 2\nu\left(\frac{\partial \sqrt{k}}{\partial r}\right)^2;\qquad \bar{v}_z = 0. \tag{9}$$

3.2. Model formulation for the dispersion

Consider the case of a fluid in fully developed turbulent flow containing a potentially reactive species and flowing through a tube of finite length. An arbitrary-order chemical reaction starts as soon as the fluid enters the test section. In the case of pipe flow, the radial profile of axial velocity (different intensity of motion at different radial locations) results in axial mixing or residence time distribution. The radial diffusion (both molecular and eddy) plays an important role in the radial homogenization of solutes, particularly in the near-wall region. The combined effect of convection and diffusion can be written by the following transient mass balance equation:

$$\frac{\partial \bar{c}}{\partial t} + \frac{1}{r}\frac{\partial}{\partial r}(r\bar{c}\,\bar{v}_r) + \frac{\partial}{\partial z}(\bar{c}\,\bar{v}_z) = \frac{1}{r}\frac{\partial}{\partial r}\left(r(D_m + D_{rr})\frac{\partial \bar{c}}{\partial r}\right) + \frac{\partial}{\partial z}\left((D_m + D_{zz})\frac{\partial \bar{c}}{\partial z}\right) + \frac{1}{\rho}R_A \tag{10}$$

In one dimensional pipe flow, we can neglect the radial component of mean velocity. Ekambara and Joshi [8] have shown

that the contribution of D_{zz} was negligible to the extent of axial mixing. Therefore, for the applicability of k–ε model, we can assume that $D_{rr} = D_{zz} = D_t$. With these simplifications, Eq. (10) takes the following form:

$$\frac{\partial \bar{c}}{\partial t} + \frac{\partial(\bar{c}\,\bar{v}_z)}{\partial z} = \frac{1}{r}\frac{\partial}{\partial r}\left(rD_{\text{eff}}\frac{\partial \bar{c}}{\partial r}\right) + \frac{\partial}{\partial z}\left(D_{\text{eff}}\frac{\partial \bar{c}}{\partial z}\right) + \frac{1}{\rho}R_A \tag{11}$$

where D_{eff} is the combined effect of molecular and eddy diffusion. It may be emphasized that $\bar{v}_z$ is not a function of z and it can be taken out of derivative sign. However, $\bar{v}_z$ is a function of r and the actual radial profile of $\bar{v}_z$ has been found using low Reynolds number k–ε model which is described in the previous section. The resulting profile of mean axial velocity ($\bar{v}_z$) has been substituted in Eq. (11).

For an arbitrary-order homogeneous reaction we have

$$R_A = -k_n \rho^n \bar{c}^n \tag{12}$$

The reaction has been considered to be thermally neutral and the temperature is assumed to be uniform throughout the reactor.

Substituting Eq. (12) into Eq. (11) will give, after rearranging,

$$\frac{\partial \bar{c}}{\partial t} + \frac{\partial(\bar{c}\,\bar{v}_z)}{\partial z} = \frac{1}{r}\frac{\partial}{\partial r}\left(rD_{\text{eff}}\frac{\partial \bar{c}}{\partial r}\right) + \frac{\partial}{\partial z}\left(D_{\text{eff}}\frac{\partial \bar{c}}{\partial z}\right) - K\bar{c}^n\left(\frac{U}{a}\right) \tag{13}$$

where we defined a homogeneous reactor constant as

$$K = \frac{k_n \rho^{n-1} a}{U} \tag{14}$$

The dispersion of the tracer is expressed by the transient mass balance (Eq. (13)). The effective diffusion coefficient, D_{eff}, is given by:

$$D_{\text{eff}} = D_m + D_t \tag{15}$$

where D_m is the molecular diffusion coefficient and D_t is the eddy diffusion coefficient. D_m and D_t are estimated by

$$D_m = \frac{\nu}{Sc} \tag{16}$$

$$D_t = \frac{\nu_t}{Sc_t} \tag{17}$$

where Sc and Sc_t are the molecular and turbulent Schmidt numbers, respectively. The latter is assumed to be 0.9 [18].

Boundary conditions:

The solution to the diffusion–convection Eq. (13) must satisfy the following boundary conditions:

$$\bar{c}(r, z, 0) = C_0$$
$$\frac{\partial \bar{c}(0, z, t)}{\partial r} = \frac{\partial \bar{c}(a, z, t)}{\bar{c}r} = 0 \quad \text{for all } z \text{ and } t. \tag{18}$$

4. Method of solution

The mathematical model was solved in two steps. In the first step, equations of continuity and motion were solved for getting the profiles of the mean axial velocity, the turbulent kinetic energy (k) the turbulent energy dissipation rate (ε) and eddy diffusivity (D_t). In the second step the flow and eddy diffusivity information obtained from step one was used for solving Eq. (13) to give concentration profiles. The radial profiles of velocity and eddy diffusivity were assumed to be independent of axial location as the flow is fully developed.

The set of equations was solved numerically, which consisted of the following steps: (i) the generation of grid, (ii) the conversion of governing equations into algebraic equations, (iii) the selection of discretization scheme, (iv) the formulation of discretized equations at every grid location and (v) the development of a suitable iterative scheme for the use in obtaining the final solution.

The finite control volume technique proposed by Patankar [19] was used for the solution of differential equations. The UPWIND scheme was used for discretization. The set of algebraic equations obtained after discretization was solved by TDMA. The grid generation is one of the important aspects of the numerical simulation. The robustness of any numerical code depends on the effectiveness and stability of the grid-generation scheme employed for investigation. Ekambara and Joshi [8] have investigated the effect of grid size in radial and axial direction. They have observed no effect of grid size beyond 100×1000, and therefore, the same number was selected in this work. Further, they also investigated the effect of time step, and they observed no effect of time step below 0.2 s. In view of these observed effects of grid size and time step, all the simulations have been carried out by using the grid size of 100×1000 and the time step of 0.2 s. Residence time distribution curves were obtained over a wide range of Reynolds numbers. These curves were used for the estimation of axial dispersion parameter. The average solute concentration is given by:

$$C = \frac{1}{\pi a^2}\int_0^a 2\pi \bar{c} r \, \mathrm{d}r. \tag{19}$$

5. Results and discussion

5.1. Comparison of flow and axial mixing predictions with experimental data

In order to test the accuracy of predictions as a result of flow simulation, an extensive comparison was made with the experimental data of Durst et al. [5]. This data set can be considered as the most accurate set among those reported in the published literature to the date. The comparison of the predicted mean axial velocity as a result of simulation ($Re = 7442$) using models of universal velocity profile, Flint [20] and the present CFD model is shown in Fig. 1. The universal mean axial velocity profile can be observed to have large deviations in the buffer and bulk regions. The CFD model exhibited an excellent comparison with the experimental data of Durst et al. [5] in the region $0.5 < y^+ < 100$.

Unlike the measurements of flow quantities, such as the mean velocity and Reynolds stresses, the accurate experimental data on the concentration profiles are scarce. Further, there are very few cases where measurements are reported for a wide range of

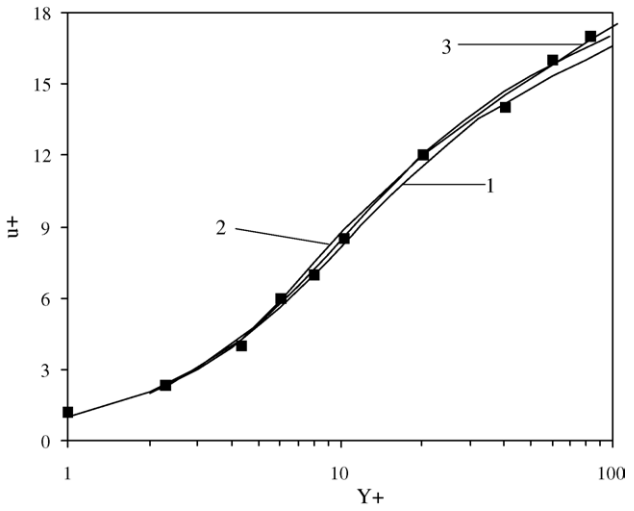

Fig. 1. Comparison of mean velocity profiles with experimental data. (■) Experimental data of Durst et al. [5], (1) universal velocity profile, (2) flint [20] and (3) CFD at $Re = 7442$.

Schmidt number. Fig. 2 depicts the comparison of the predicted residence time distribution (RTD) curve ($Re = 3810$, $Sc = 1$) with the experimental data of Flint and Eisenklam [21]. It can be seen that the predicted and experimental concentration profiles are in excellent agreement. Further, Ekambara and Joshi [8] extended the model to predict the residence time distributions over a wide range of Re (2500–10^6), Sc (0.27–1.0) and pipe diameter (0.0254–0.0508 m).

5.2. CFD simulation of homogeneous reactions

In view of the success of prediction of velocity profile and residence time distribution, the model has been extended to see the effect of arbitrary reaction orders and various reaction rate constants on the axial and radial concentration profiles. A typical results are shown in Fig. 3 in terms of axial profile of average

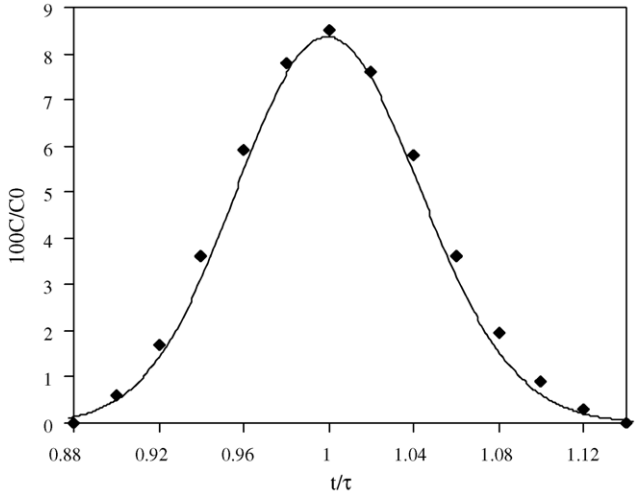

Fig. 2. Comparison between the predicted concentration profile and the experimental data. (—) CFD and (♦) experimental data of Flint and Eisenklam [21] at $Re = 3810$, $Sc = 1$.

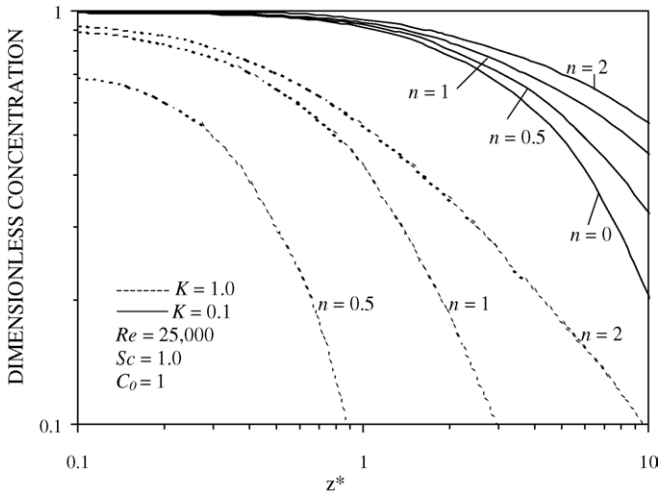

Fig. 3. Effect of reaction orders on the longitudinal average concentration distribution.

(cross-sectional) concentration. The figure shows that the effect of increasing reaction order results into a decrease in conversion. Further, as the rate constant increases the effect of reaction orders on the axial concentration distribution becomes highly pronounced.

Fig. 4 shows the effect of increasing the reaction rate constant on average and center-line concentrations as a function of the downstream aspect ratio. Increasing the reaction rate constants obviously increases the rate of consumption of the reactant. For $K = 0.001$, there exists some difference between the average and the center-line concentrations. The difference becomes highly noticeable for large values of the aspect ratio, but beyond a certain aspect ratio, both the concentrations decrease at an approximately identical rate. Most of the difference is due to the reactant in the immediate vicinity of the wall region. Here, because of substantial decrease in velocity and a corresponding increase in residence time, a greater level of conversion can be achieved, resulting in a lower average concentration. However, at very high rate constant values even the concentration in the bulk of the fluid depletes at a rapid rate, so that after a certain down-

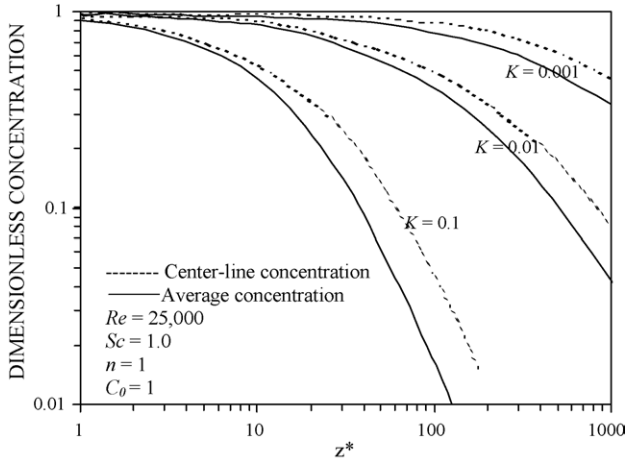

Fig. 4. Effect of dimensionless rate constants on the longitudinal average and center-line concentration distributions.

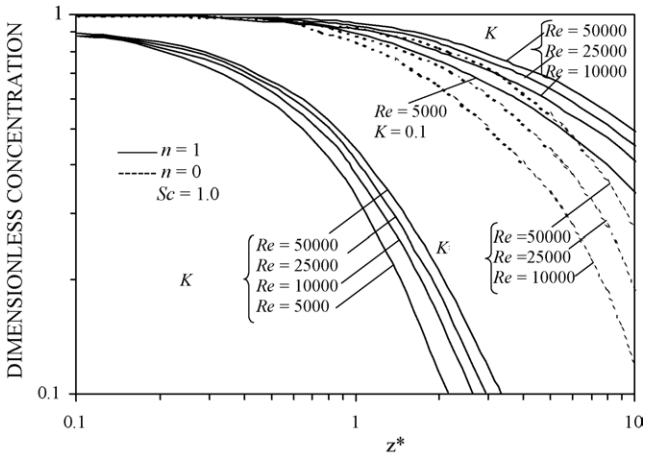

Fig. 5. Effect of Reynolds number on the longitudinal average concentration distribution.

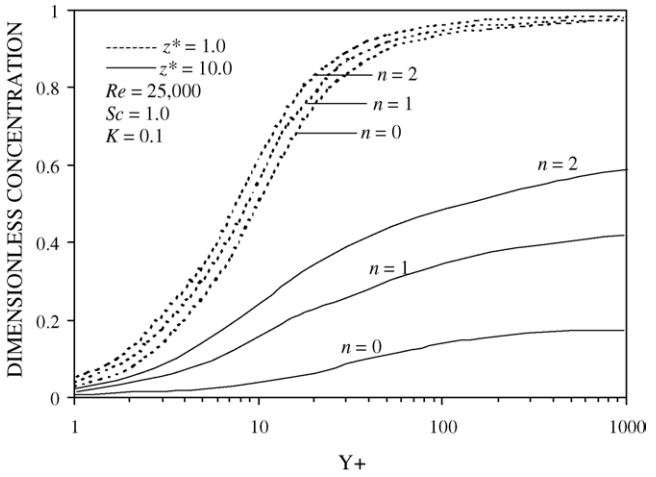

Fig. 6. Radial concentration profiles for various reaction orders and two downstream aspect ratios.

stream distance subsequent contributions from the wall region are of relatively negligible proportions. In other words, there occurs a parallel shift downwards in the concentration profile.

The effect of Reynolds number on the degree of conversion for representative reaction orders and rate constants is shown in Fig. 5. It can be seen that, an increase in the Reynolds number would cause a decrease in the axial gradients resulting in a lower level of conversion as well as a decrease in the segregational effects. It is interesting to note that the spread due to increasing Reynolds number is not affected to any noticeable degree when the rate constant increases.

Changes in reaction order do cause a substantial change in the spread due to increasing Reynolds number. As can be seen, the effect of changing the Reynolds number from 10,000 to 50,000 is far more pronounced and significant in the average concentration for a zero-order reaction than for a first-order reaction. For a second-order reaction the effect can be seen to be too small to be considered. It was noticed, but not indicated in the figure, that the difference between the average and center-line concentrations was consistently greater for $Re = 10{,}000$ than for $Re = 50{,}000$. This can readily be accepted because at $Re = 50{,}000$ a much higher level of turbulence and a thinner wall region tend to average the concentrations more uniformly. Also, radial gradients are considerably less pronounced, further averaging the concentrations.

Radial concentration profiles for various reaction orders at two downstream aspect ratios are shown in Fig. 6. The distance from the wall considered in terms of the dimensionless distance y^+ permits a detailed analysis of the region adjacent to the wall. It is in this region that most of the changes occur. A study of Fig. 6 shows that substantial changes occur in the region $0 < y^+ < 20$, where a very sharp decrease in point concentrations begins for $z^* = 1$. There is a greater decrease of point concentrations over the entire range of y^+ for the zero-order reaction, followed by the first-order and then the second-order reactions. Note that at lower aspect ratios the shape of the concentration distributions is identical to the shape of the turbulent momentum profile curve. At higher aspect ratios the rate of reaction decreases sharply in the wall region of the low concentrations existing there. The

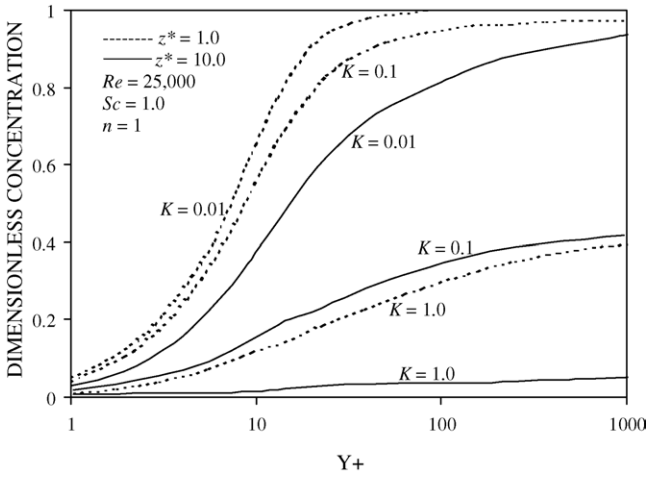

Fig. 7. Radial concentration for various dimensionless rate constants and tow downstream aspect ratios.

rate, however, is still substantial in the wall region, resulting in a general flattening profile at $z^* = 10$.

Fig. 7 shows the radial concentrations for various rate constants and two aspect ratios as a function of the dimensionless distance from the wall, y^+. As expected, an increase in the rate constant causes a decrease in the concentration profiles. The rate of decrease in concentration increases sharply with an increase in the rate constant K since the decrease is considerably more as K increases from 0.1 to 1 than from 0.01 to 0.1.

6. Conclusions

1. The low Reynolds number k–ε model of Lai and So [6] has been used to predict the liquid velocities and the turbulent viscosity. The comparison between the predictions and the experimental profiles of $\overline{v}_z$, k and D_t was found to be excellent. The model also establishes good energy balance.
2. A CFD model has been developed to analyze turbulent reactive flows in tubular non-catalytic reactors for arbitrary reaction orders and rate constants.

3. The zero-order reaction gives the maximum conversion for a particular downstream aspect ratio. The degree of conversion decreases, respectively, for first- and second-order reactions. Changes in radial concentrations show that, at low aspect ratios, almost all the phenomena occur adjacent to the wall. It is only when the concentration near the wall gets very low, causing a rapid decrease in the rate of reaction, that the concentration in the core decreases more rapidly in relation to that in the wall region.
4. An increase in Reynolds number generally decreases the amount of reactant consumed. With an increase in Schmidt number, however, the amount of reactant consumed shows a corresponding increase.

Acknowledgements

Two of us (Ekambara and Dhotre) acknowledge the fellowship support given by the University Grants Commission (UGC), Government of India.

References

[1] V.C. Patel, W. Rodi, G. Scheuerer, Turbulence models for near wall and low Reynolds number flows, Rev. AIAA J. 23 (1985) 1308–1319.
[2] C.M. Hrenya, E.J. Bolio, D. Chakrabarti, J.L. Sinclair, Comparison of low Reynolds number k–ε turbulence model in predicting fully developed pipe flow, Chem. Eng. Sci. 12 (1995) 1923–1941.
[3] S.S. Thakre, J.B. Joshi, CFD modelling of heat transfer in turbulent pipe flows, AIChE J. 46 (2000) 1798–1812.
[4] S.S. Thakre, J.B. Joshi, Momentum, mass and heat transfer in single-phase turbulent flow, Rev. Chem. Eng. 18 (2002) 83–293.
[5] F. Durst, J. Jovanovic, J. Sender, LDA measurements in the near-wall region of a turbulent pipe flow, J. Fluid Mech. 295 (1995) 305–335.
[6] Y.G. Lai, R.M.C. So, On near wall turbulent flow modeling, J. Fluid Mech. 221 (1990) 641–673.
[7] S.S. Thakre, J.B. Joshi, Low Reynolds number k–ε modeling: flow patterns and energy balance, Can. J. Chem. Eng. 78 (2001) 214–226.
[8] K. Ekambara, J.B. Joshi, Axial mixing in pipe flows: transition and turbulent regions, Chem. Eng. Sci. 58 (2003) 2715–2724.
[9] R.D.L. Bosworth, Philos. Mag. 39 (1948) 847.
[10] K.G. Denbigh, The kinetics of continuous reaction processes: application to polymerization, J. Appl. Chem. 1 (1951) 227–236.
[11] F.A. Cleland, R.H. Wilhelm, Diffusion and reaction in viscous flow tubular reactor, AIChE J. 2 (1956) 489–497.
[12] S. Krongelb, M.W.P. Strandberg, Use of paramagnetic resonance techniques in the study of atomic oxygen re-combinations, J. Chem. Phys. 31 (1959) 1196–1210.
[13] H.A. Lauwerier, A diffusion problem with chemical reaction, Appl. Sci. Res. A8 (1959) 366.
[14] E.H. Wissler, R.S. Schechter, A diffusion problem with chemical reaction, Appl. Sci. Res. A10 (1961) 198.
[15] J.P. Vignes, P.I. Trambouze, Diffusion et rĕaction chimique dans un reacteur tubulaire en rĕgime laminaire, Chem. Eng. Sci. 17 (1962) 73–86.
[16] C.J. Hsu, A method of solution for mass transfer with chemical reaction under condition of viscous flow in a tubular reactor, AIChE J. 11 (1965) 938–940.
[17] W.M. Edwards, D.I. Saletan, Applied Kinetics and Chemical Reaction Engineering, ACS Publications, Washington, 1967, p. 133.
[18] A.J. Reynolds, The prediction of turbulent Prandtl and Schmidt number, Int. J. Heat Mass Transfer 18 (1975) 1055–1069.
[19] S.V. Patankar, Numerical Heat Transfer and Fluid Flow, McGraw-Hill, New York, 1980.
[20] L.F. Flint, On the velocity profile for turbulent flow in straight pipe, Chem. Eng. Sci. 22 (1967) 1127–1131.
[21] L.F. Flint, P. Eisenklam, Longitudinal gas dispersion in transitional and turbulent flow through a straight tube, Can. J. Chem. Eng. 47 (1969) 101–106.